# Competition between ferromagnetism and frustrated antiferromagnetism in quasi 2D $Ce_{2.15}(Pd_{1-x}Ag_x)_{1.95}In_{0.9}$ alloys



2016 J. Phys.: Condens. Matter 28 475601

(http://iopscience.iop.org/0953-8984/28/47/475601)

IOP Publishing Journal of Physics: Condensed Matter

J. Phys.: Condens. Matter **28** (2016) 475601 (8pp) doi:10.1088/0953-8984/28/47/475601

# Competition between ferromagnetism and frustrated antiferromagnetism in quasi 2D $Ce_{2.15}(Pd_{1-x}Ag_x)_{1.95}In_{0.9}$ alloys

**J G Sereni[1,4], M Giovannini[2,3], M Gómez Berisso[1] and F Gastaldo[2]**

[1] Low Temperature Div. CAB—CNEA, Conicet, 8400 Bariloche, Argentina
[2] Dip. di Chimica e Chimica Industriale, Università di Genova, I-16146 Genova, Italy
[3] CNR-SPIN Corso Perrone 16152 Genova, Italy

E-mail: jsereni@cab.cnea.gov.ar

Received 20 June 2016, revised 10 August 2016
Accepted for publication 17 August 2016
Published 16 September 2016

**Abstract**

Low temperature thermal and magnetic measurements performed on ferro-magneticl (FM) alloys of composition $Ce_{2.15}(Pd_{1-x}Ag_x)_{1.95}In_{0.9}$ are presented. Pd substitution by Ag depresses $T_C(x)$ from 4.1 K down to 1.1 K for $x = 0.5$, which is related to the increase of band electrons, with a critical concentration extrapolated to $x_{cr} \approx 0.6$. The $T_C(x)$ decrease is accompanied by a weakening of the magnetization of the FM phase. At high temperature ($T > 30$ K) the inverse magnetic susceptibility reveals the presence of robust magnetic moments ($2.56 \geqslant \mu_{eff} \geqslant 2.4\,\mu_B$), whereas the low value of the Curie–Weiss temperature $\theta_P \approx -10$ K excludes any relevant effect from Kondo screening. The specific heat jump at $T_C(x)$ decreases accordingly, while an anomaly emerges at a fixed temperature $T^* \approx 1$ K. This unexpected anomaly does not show any associated sign of magnetism checked by AC-susceptibility measurements. Since the total magnetic entropy (evaluated around $T = T_C(x = 0)$) practically does not change with Ag concentration, the transference of degrees of freedom from the FM component to the non-magnetic $T^*$ anomaly is deduced. The origin of this anomaly is attributed to an arising magnetic frustration of the ground state and the consequent *entropy bottleneck* produced by the divergent increasing of density of excitations at low temperature.

Keywords: magnetic frustration, cerium compounds, specific heat, entropy

(Some figures may appear in colour only in the online journal)

## 1. Introduction

There is an increasing number of rare earth compounds recently studied which do not show magnetic order (MO) down to low temperature ($T \leqslant 1$ K) despite the fact that their ground states exhibit robust magnetic moments. They are characterized by a continuous growing of the density of low energy states reaching the value of $C_{4f}/T \approx 12$ J mol$^{-1}$ K$^{-2}$ in the specific heat of $YbPt_2In$ [1]. Another group of compounds show a characteristic $C_{4f}(T)/T$ anomaly centered around 1 K [2]. Searching for the possible origin of these behaviors one finds that atomic disorder inhibiting long range MO propagation is unlikely because their magnetic atoms lie in periodic lattices. Large interatomic spacing between magnetic atoms reducing the RKKY interaction strength can also be ruled out considering that some compounds with a large Ce–Ce interatomic distance like e.g. $CeZn_{11}$ [3] and other binary compounds order magnetically [3, 4].

The proximity to a quantum critical point (QCP) [5, 6] or geometric frustration [7] also have been considered. In contrast to the QCP scenario, there are scarce predictions about the expected thermal behavior for real frustrated systems allowing their unambiguous recognition [8]. It is therefore highly desirable to strengthen the experimental investigation of magnetically frustrated systems.

The search of this class of systems can be addressed to crystalline structures with steric atomic arrangements that favor geometric frustration like, for example, tetrahedral

[4] Author to whom any correspondence should be addressed.

 

(pyrochlore) in a three dimensional (3D) configuration, or triangular coordination of magnetic atoms with antiferromagnetic (AFM) interaction in 2D cases [7, 8]. The family of compounds $R_2TM_2X$ (where R = Rare earth, TM = Transition and X = semi metal) belongs to the latter group, offering a fertile field for such investigation [9] because of its highly anisotropic $Mo_2B_2Fe$ type structure. In this structure, magnetic and non-magnetic layers alternate along the '*c*' direction (see for example [10]), with the magnetic atoms distributed in a so called 'pin weal' quasi 2D network within the '*a,b*' plane.

In the case of the solid solution $Ce_{2\pm x}Pd_{2\mp y}In_{1-z}$ [11], ferromagnetic (FM) or AFM phases form depending on the relative concentration of *electron* (FM)/ *holes* (AFM) in the TM-X layer [12]. In FM alloys, the electronic concentration is increased by an excess of Ce in the TM-X layer mainly substituting In atoms but also Pd ones. There is, however, an exception to this dependence observed in $Ce_{2.15}Pd_{1.95}In_{0.9}$ alloys doped with Ag because their $T_C(x)$ decrease despite of the *electron*-like character of the dopant [13]. This apparently contradictory behavior of Ag doped alloys in comparison to isotypic alloys with other TM elements was tentatively attributed to an arising magnetic frustration. To our knowledge, most of geometrically frustrated systems are reported in stoichiometric compounds [7–9, 14]. However, in the system at hand the frustration character increases with Ag content. In this work we present a more extended investigation of this system by doubling the number of alloys in comparison to a preliminary study published elsewhere [13], after an accurate characterization of its structural properties and samples quality. New and more detailed results allows to get insight on the magnetization properties and entropy evolution with Ag content. The origin and the nature of the unexpected anomaly that emerges around 1 K are here discussed in detail within the phenomenology characterizing frustrated system. A new physical concept of 'entropy bottleneck' is introduced in order to explain how the third law of thermodynamics controls the $T \to 0$ dependence of the entropy. The effect of external magnetic field on the specific heat of the most representative alloy ($x = 0.5$) is also presented.

## 2. Experimental details and results

### 2.1. Compounds formation and characterization

A series of polycrystalline samples with nominal compositions $Ce_{2.15}(Pd_{1-x}Ag_x)_{1.95}In_{0.9}$ with $x = 0,0.1,0.2,0.3,0.4,0.5,0.6,0.7,0.8$ were prepared by argon arc melting the elements on a water cooled copper hearth with a tungsten electrode. The starting materials were indium (ingot, 99.999 mass% purity, Johnson Matthey, Karlsruhe, Germany), cerium (rod, 99.9 mass% purity, NewMet Kock, Waltham Abbey, UK), palladium and silver (sheets, 99.95 mass % purity, Chimet, Arezzo, Italy). To ensure good homogeneity the buttons were turned over and remelted several times. Weight losses after melting were generally smaller than 0.5 mass %. All the alloys were then annealed in a resistance furnace at 750 ° C for 168 h and finally water quenched. Scanning electron microscopy (SEM), and electron probe micro-analysis (EPMA) based on

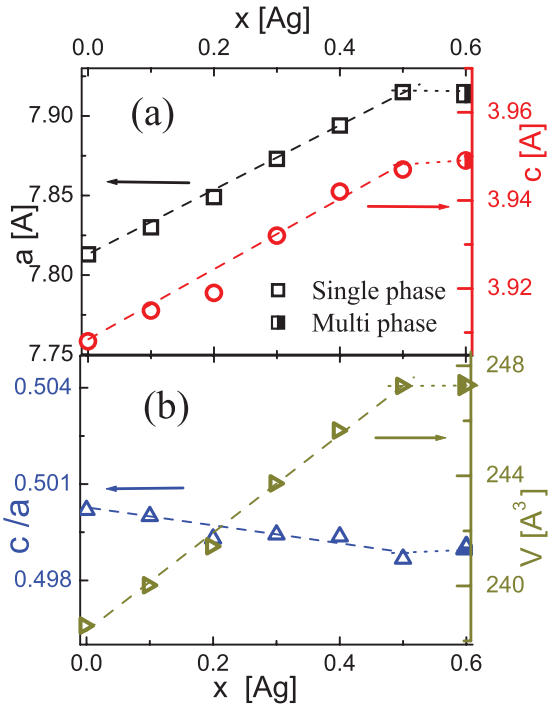


**Figure 1.** (a) Lattice parameter variation as a function of Ag content up to the limit of solubility $x = 0.5$. Structural parameters for $x = 0.6$ are included to show the saturation values of the lattice parameters. Dashed lines are guides to eye. (b) Nearly constant *c/a* ratio and unit cell volume dependence. Dashed lines are also guides to the eye.

energy-dispersive x-ray spectroscopy were used to examine the actual phase compositions. The compositional contrast was revealed in unetched samples by means of a backscattered electron detector (BSE). The composition values derived are usually accurate to 1 at%. X-ray diffraction (XRD) was performed on powder samples using a vertical diffractometer X-Pert with Cu $K_\alpha$ radiation. The equipments used for measuring specific heat and magnetization were described elsewhere [12].

All the $Ce_{2.15}(Pd_{1-x}Ag_x)_{1.95}In_{0.9}$ alloys are almost single phase (with phase compositions coincident with synthesis compositions within the EPMA errors) crystallizing in the $Mo_2B_2Fe$-type structure up to the limit of solubility of around $x = 0.5$, as shown from the trend of lattice parameters of figure 1. In fact, lattices parameters a and c increase proportionally to the substitution of Pd by the bigger Ag following Vegard's law up to saturation of the values at around $x = 0.5$ (dashed lines). The structural parameters for $x = 0.6$ are included in the figure to make evident the limit of the single phase range through the saturation of the lattice parameters values. Besides this phase, traces of $Ce_3In$ are present in some of the samples throughout the solid solution, whereas sample $x = 0.5$ presents traces of an unknown phase of per cent composition $Ce_{36}Ag_{39}In_{25}$.

### 2.2. Magnetic properties

The magnetic susceptibility results follow a modified Curie–Weiss law $\chi(T) = \chi_{cw}(T) + \chi_P$ above ≈30 K, where a temperature and nearly concentration independent Pauli-like

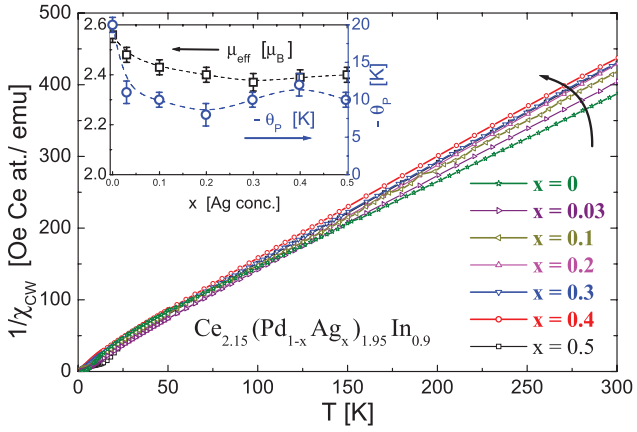


**Figure 2.** Inverse of the Curie–Weiss contribution to the magnetic susceptibility, measured in a field of 0.5 T is shown after the Pauli-type contribution subtraction. The increase of Ag concentration is indicated by the arrow. Inset: Ag concentration dependence of the Ce effective moment (left axis) and paramagnetic temperature (right axis).

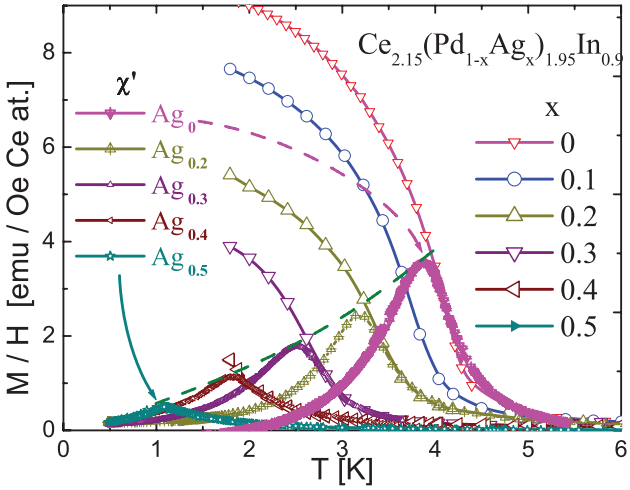


**Figure 3.** Thermal dependence of the magnetization at low temperature measured with $H = 0.01$ T showing the typical behavior of a FM system. The inductive component of AC-susceptibility ($\chi'(T)$) is included after scaling them with respective $M(T)/H$ values. The results for $x = 0.1$ are not included for clarity. The $\chi'$ maxima mark the $T_C(x)$ temperatures that show a nearly linear decrease (dashed line) with Ag content.

contribution $\chi_P$ is included. From the inverse of $\chi_{cw} = \frac{Cc}{T+\theta}$ (see figure 2) the Curie constant ($Cc$) is obtained which, for the pure Pd alloy, indicates the presence of a $Ce^{3+}$ moment $\mu_{eff} = 2.56\ \mu_B$/Ce at. The $\chi_{cw}(T)$ values included in the figure were obtained after subtracting a $\chi_p = (2 \pm 0.5)10^{-4}$ emu/Ce at.Oe contribution. In the inset of figure 2 its concentration dependence is shown to slightly decrease down to ≈2.4 $\mu_B$ at $x = 0.5$. The Curie–Weiss temperature $\theta$ practically does not change with Ag concentration, remaining around $\theta \approx -10$ K as depicted in the inset of figure 2. Below that temperature, the reduction of the crystal electric field states population is reflected in a downward curvature, which agrees with the FM character of the ground state (GS).

The low temperature dependence of the magnetization $M(T)$ was measured applying a field $H = 0.01$ T in a field cooling process. Those results are presented as a $M/H$ ratio in figure 3. Again, the FM character of the GS shows up as an upturn of $M(T)/H$ at $T \leqslant 4$ K, but with a magnetization signal decreasing proportionally to $T_C(x)$.

Magnetic measurements were extended from $T = 1.8$ K, down to 0.5 K using AC-susceptibility ($\chi'$) techniques. These results are included in figure 3, where the weakening of the $\chi'$ signal proportionally to $T_C(x)$ can be observed. The $T_C(x)$ temperature is identified with the maximum of $\chi'(T)$ that coincides with the maximum of the $\partial M/\partial T < 0$ slope. Despite of the $\chi'(T,x)$ decrease, the results from sample $x = 0.5$ still indicate the presence of a very weak transition at $T_C = 1$ K.

Magnetization $M(H)$ measurements at $T = 1.8$ K are shown in figure 4. Samples $x = 0.1$ and 0.2 show a rapid increase at low field, reaching about 90% of the estimated saturation value $M_{sat} \approx 1.1\ \mu_B$/Ce at. at $H \approx 0.5$ T. $M_{sat}$ was estimated using a simple approximation for $M(H) = M_{sat} - a/H + b/H^2$. Above these concentrations ($x \geqslant 0.3$), the initial $M(H)$ slope weakens and transforms into a continuous curvature dependence. Nevertheless, a decreasing hysteresis loop is observed between $-0.3 < H < 0.3$ T, as shown in the inset of figure 4 for $x = 0.3$ and 0.5. This remanent hysteresis in sample $x = 0.5$ suggests the presence of two contributions at this concentration. One is the vanishing, but still present, FM component and another of paramagnetic character containing quite robust Ce moments. This unusual scenario is confirmed by a fit performed on the $M(H)$ curve of sample $x = 0.5$ (see the continuous curve in figure 4) using a paramagnetic Langevin function with an offset of 0.21 $\mu_B$/Ce at. accounting for the hysteresis loop contribution.

### 2.3. Specific heat

The magnetic contribution to the specific heat ($C_m$) is obtained after subtracting the phonon contribution extracted from the $La_2Pd_2In$ compound. The FM transition manifests itself as a jump $\Delta C_m$ which for $x = 0$ is ≈10 J/Ce at. K (see figure 5), close to the mean field prediction for a doublet GS [15]. Below $T_C$, the positive curvature of $C_m(T)$ is properly described by an exponential function of the type $C_m(T) = [0.12 + 2 * T * e^{-\Delta/T}]$ J molK$^{-1}$, which reveals a gap $\Delta = 1.9$ K in the magnon spectrum as it is typically observed in strongly anisotropic systems.

Increasing Ag concentration, the $\Delta C_m$ jump broadens and progressively decreases its intensity inline with the $\partial M/\partial T|_{T_C}$ slope decrease. Unexpectedly, an anomaly centered at $T^* \approx 1$ K emerges and overcomes the FM $\Delta C_m/T$ jump around $x = 0.3$, without changing its temperature position. At the $x = 0.5$ concentration limit, this anomaly seems to be fully developed (see the inset in figure 6 on the right axis).

A $C_m(T)/T$ representation, presented in figure 5, reveals a clear transference of degrees of freedom between two competing components in the system, one associated to the decreasing FM contribution and the other to the emerging $T^* \approx 1$ K anomaly. The arising anomaly overcomes the FM maximum around $x = 0.3$, making a quantitative distinction between those similar contributions a little difficult at

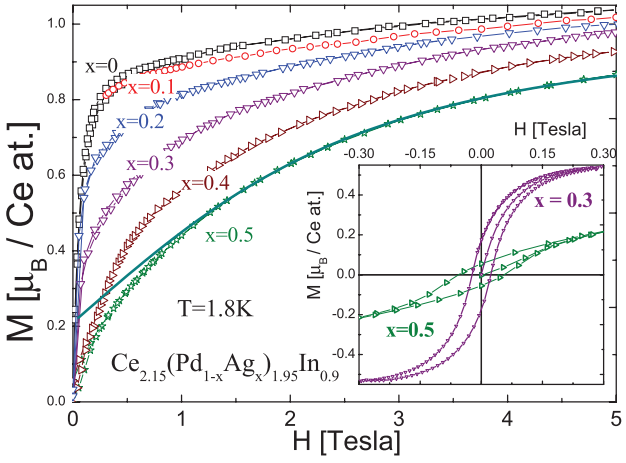


**Figure 4.** Magnetization curves of all studied samples as a function of applied field. Continuous curve: fit for sample $x = 0.5$ with a Langevin function with a FM offset. Inset: detail of the hysteresis loops at low field in sample $x = 0.5$ compared with sample $x = 0.3$.

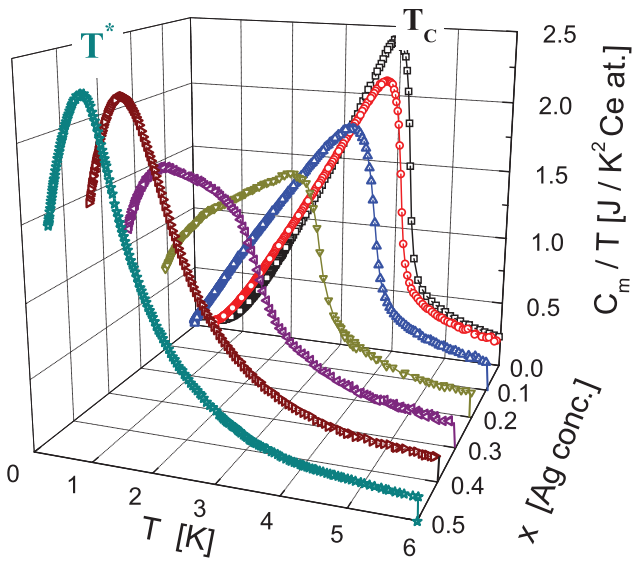


**Figure 5.** Magnetic contribution to the specific heat of $Ce_{2.15}(Pd_{1-x}Ag_x)_{1.95}In_{0.9}$ alloys in a 3D representation, showing a vanishing FM transition and an emerging anomaly around 1 K.

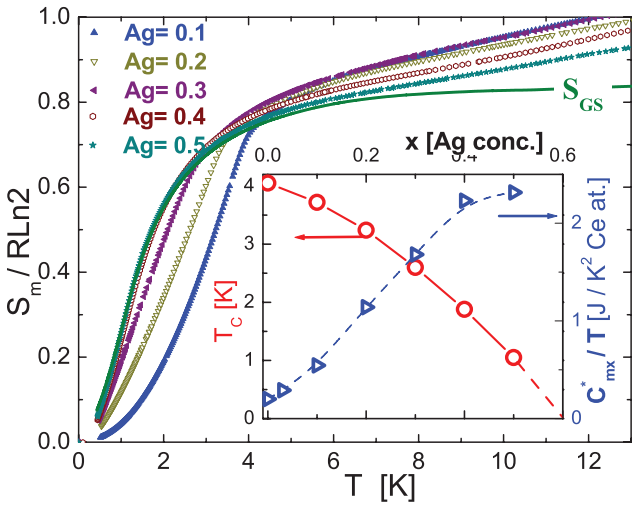


**Figure 6.** Entropy gain for all studied alloys normalized to a doublet GS per Ce atom. Continuous curve: $S_{GS}$, entropy saturation for sample $x = 0.5$ after CEF levels contribution subtraction. Inset, left axis (red circles): magnetic phase diagram showing $T_C(x)$ extracted from the maximum of $\chi'$ for $x \geqslant 0.2$. Right axis (blue triangles): $C_m/T$ value at $T = T^*$.

intermediate Ag concentrations. This anomaly cannot be associated to a Schottky ($C_{sh}$) like or a standard spin glass ($C_{sg}$) specific heat anomaly because the former has a maximum value of $C_{sh}(T)$ which depends on the relative degeneration of the ground and the excited states [16], not fitting into the present experimental results. The latter requires an associated magnetic signal related to the internal field which changes with Ag concentration with the consequent variation of the temperature position of $C_{max}$. Concerning the thermal variation, none of the mentioned anomalies fit into the observed $C_m(T)/T$ dependence of the present '1 K' anomaly. In fact, on the $T \ll T^*$ limit, spin glasses are expected to show a constant $C_{sg}/T$ value [17] whereas the Schottky anomaly to grow exponentially $C_{sh} \propto e^{(-\Delta/T)}$ [16], both clearly different from the $C_m/T \propto T$ observed in sample $x = 0.5$. At high temperature (i.e. $T \gg T^*$) the specific heat of those anomalies decay as $C_p/T \propto 1/T^3$ [15], also differently than the $C_p/T \propto 1/T^2$ observed in this compound (see figure 9).

Before to analyze the entropy evolution of this systems it is convenient to determine at which temperature the first excited doublet of crystal electric field (CEF) starts to contribute to $C_m(T)$. For such a purpose the CEF splitting was evaluated by fitting the $C_m(T)$ data extracted from sample $x = 0.5$ up to 20 K (not shown). The procedure, previously used to analyze similar results [18], applies a set of Schottky anomalies which allows to mimic the profile of the distribution of states along the energy and the levels broadening produced by an eventual Kondo effect. As a result, a splitting of $\Delta_I = 52$ K with a broadening of 10 K $\propto T_K$ was obtained. Both results are in good agreement with previous estimation of $\Delta_I = 60$ K for the $x = 0$ compound [12]. This analysis guaranties that only a doublet is involved in the GS properties at the $T \leqslant T_C$ range. The upper limit of our specific heat measurements ($T = 20$ K) does not allow to evaluate the splitting of the second CEF excited doublet.

### 2.4. Entropy gain

The entropy gain $S_m(T)$, normalized to $R \ln 2$ for a doublet GS, is shown in figure 6. At low temperature one can appreciate how the positive curvature of $S_m(T < T_C)$, related to the FM phase, progressively vanishes with Ag content. Two important features are observed at $T > T_C(x = 0) = 4.1$ K: (i) the isothermal entropy decreases with concentration by about a 10% at e.g. $T = 10$ K, between $x = 0$ and 0.5, and (ii) above $T \approx 7$ K an incipient contribution of the first CEF excited level sets on. The pure entropic contribution of the GS ($S_{GS}$) for sample $x = 0.5$, evaluated after subtracting the CEF contribution to the $S_m(T)$, is also included in figure 6 as a continuous curve $S_{GS}(T)$ that tends to saturate at ≈84% of $R \ln 2$. This deficit of entropy will be discussed in the context of magnetic frustration effects in the next section together with the magnetic nature and the origin of the '1 K' anomaly.

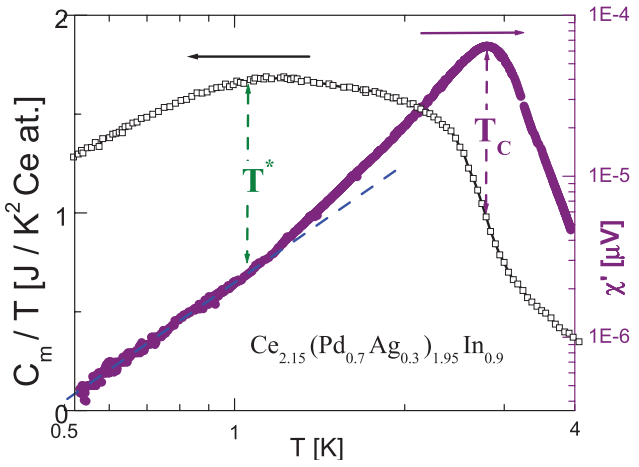


**Figure 7.** Comparison between $\chi'_{AC}(T)$ (right axis) and $C_m/T(T)$ (left axis) of sample $x = 0.3$. The arrow (green) at $T^* \approx 1$ K compares the position of the maximum of the $C_m/T$ anomaly with the absence of the $\chi'_{AC}(T)$ anomaly at that temperature. The arrow (red) at $T_C = 2.8$ K compares the $C_m/T$ jump and the $\chi'_{AC}$ maximum at $T = T_C$. Notice the logarithmic scale for $T$ and $\chi'_{AC}$. The dashed line is a guide to the eyes.

The inset of figure 6 represents a schematic magnetic phase diagram, containing the two representative parameters of the physical evolution of this system as a function of Ag doping: the MO temperature $T_C(x)$ and the $C^*_{max}(x)$ of the '1 K' anomaly. As mentioned before, the trend of these Ag doped alloys contradicts the general tendency of the $Ce_2Pd_2In$ family concerning the increase (decrease) of the number of band electrons in the Pd-X layer that favors a FM (AFM) GS [12, 19]. Such a controversy suggests that another factor, rather than the mentioned electronic concentration related to the Fermi energy, dominates the physical behavior of this system.

## 3. Discussion

A relevant information obtained from $\chi'(T)$ results is represented in figure 7 for sample $x = 0.3$. In this figure a decrease of the magnetic response below $T_C$, without any magnetic anomaly around $T^* \approx 1$ K, is observed. Despite the fact that the $\chi'(T)$ signal (presented in $\mu$V units, as measured) covers more than two decades from its highest value at $T_C = 2.7$ K, it decreases monotonously down to the lowest limit of measurement ($T \approx 0.5$ K). On the other hand, the growing specific heat anomaly at $T^*$ (also included in the figure for comparison) shows that there is a similar amount of degrees of freedom of FM and '1K' anomaly components in that alloy. The absence of magnetic signal around $T^*$ is an unexpected feature and one of the outstanding aspect of this system. To our knowledge, there is no antecedent for any low temperature specific heat anomaly arising in a system with robust magnetic moments without showing an associated magnetic response.

Atomic disorder in the Pd/Ag plane cannot be argued as a relevant factor for the origin of this anomaly because the difference of the atomic size between these two neighboring elements is only about 4%. Furthermore, an increasing atomic disorder usually drives a magnetic system from long range

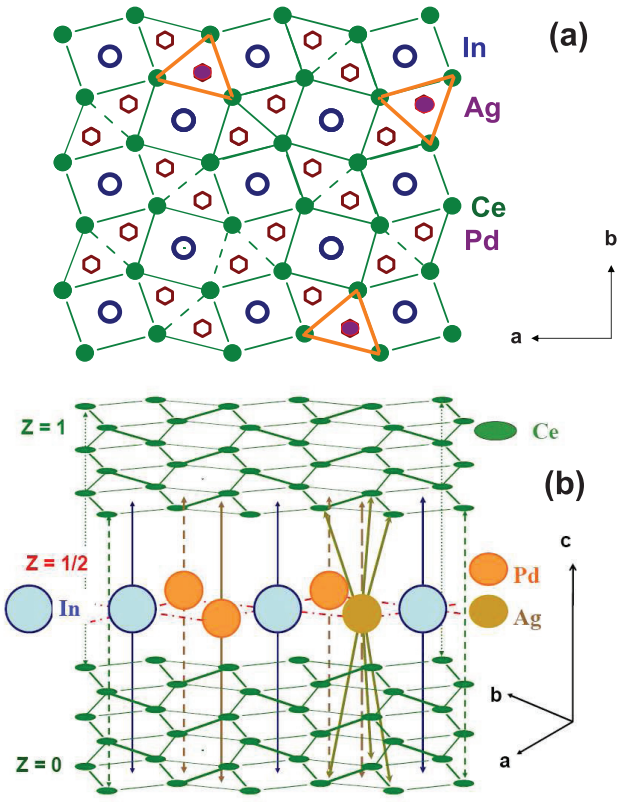


**Figure 8.** Schematic representation of the crystal structure of $Ce_2Pd_2In$. (a) Structure projection on the '$a$, $b$' plane. Full circles indicate random positions of doping (Ag) atoms in open (Pd) positions, projected into a Ce triangular neighboring coordination. (b) View of the magnetic Ce-planes intercalated with non-magnetic In and Pd (Ag) atoms. The position of a doping atom (Ag) is connected to its Ce-*nn* by three arrows in respective directions.

MO into a short range type of MO in a continuous manner, but without suppressing the total magnetic signal at all, unless e.g. a Kondo mechanism takes over. The broadening of the FM transition observed in figure 5 is typically explained by a progressive degradation of the FM order parameter along the magnetic atoms positions, that can be visualized as a tendency to clustering or spin glass behavior. Nevertheless, this description does not apply to this system because such evolution would involve a single $C_m(T)/T$ anomaly, whereas in this case one sees one (FM) contribution decreasing in intensity and temperature while the other emerges at fixed temperature ($T^*$) as Ag concentration increases. Magnetic field effect, discussed in the following section and presented in figure 9 confirms this behavior.

The microscopic coexistence of FM ordered and frustrated states can be visualized taking into account that the long range FM order parameter degradation is produced (at low Ag concentration) by the presence of randomly distributed frustrated islands. Those single AFM frustrated triangles percolate with Ag concentration increase. This scenario resembles that of a growing non magnetic regions. Although from our macroscopic measurements a phase separation cannot be excluded, the required interphase energy makes that topology highly unlikely since the lack of a magnetic resulting signal those AFM frustrated triangles cannot develop an ordering

parameter. It is evident that this description requires of spectrocopic observation to be confirmed.

### 3.1. Frustration effects

In order to understand the peculiar behavior of this system, one should focus on the two main questions arising from these experimental results concerning the nature and the origin of the '1 K' anomaly.

The usual scenarios able to explain the lack of magnetic response of this system, like Kondo screening and Ce-*nn* spacing, can be discarded. In fact, for the former the robust $\mu_{\rm eff}$ and low $-\theta_P(x) \propto T_K$ slightly depend on Ag concentration. For the latter, the lattice parameters increase less than 1.3% between $x = 0$ and 0.5 (see figure 1). Such a small volume variation is due to the similar size of Pd and Ag neighbor elements, that also makes any atomic disorder practically irrelevant for the neighboring Ce-layers as recently mentioned. Within this context, frustration effects represent the more likely scenario because they prevent the magnetic interactions to develop MO, without requiring the weakening of the magnetic moments nor the exchange (typically $J_{\rm RKKY}$) interaction. In fact, the triangular coordination of Ce-*nn* fulfils the condition for magnetic frustration within Ce planes [8], as depicted in figure 8(a). In addition to this geometric condition magnetic frustration requires the presence of AFM interactions.

As it was mentioned, Ag doping is expected to produce a strengthening rather than a weakening of the FM character in these family of compounds. However, analyzing the indirect interaction $J_{\rm RKKY} = J_{sf}^2 \delta(\epsilon_{\rm F}) \propto 1/r^3$ in detail, one should take into account that it depends on: (i) the on-site coupling $J_{sf}$ between conduction electrons spins ($s$) and magnetic moments ($f$); (ii) the density of states in the conduction band $\delta(\epsilon_{\rm F})$ and (iii) the distance between '$f$' moments: Ce-*nn* $\propto 1/r^3$. Since parameters (ii) and (iii) are slightly affected by Ag doping, the local $J_{sf}$ exchange emerges as the main responsible for this peculiar behavior.

The structural positions of the magnetic atoms (RE) in these compounds can be depicted as trigonal and tetragonal prisms, centered around 'T' and 'X' atoms respectively, see figure 8(b), where T = Pd or Ag and X = In. The RE atoms are located in non centro-symmetric positions along the 'c' direction, as projected on the plane 'ab' in figure 8(a). As a consequence of the trigonal disposition, one may expect a 'one to one' correlation of magnetic properties between $Ce_2T_2X$ compounds and the related CeT binary compounds [4] with CrB- or FeB-type structures (both structured in trigonal prisms [20]). From previous investigations on $Ce(Pd_{1-x}Ag_x)$ alloys exhibiting CrB-type structure [21], one learns that the substitution of a 'd-hole' Pd ligand by a 's-electron' Ag atom modifies the polarization of the $J_{\rm RKKY}$ interaction by changing the sign of the local $J_{sf}$ exchange. Therefore, the trigonal prism formed by Ce, Pd and Ag atoms in $Ce_{2.15}(Pd,Ag)_{1.95}In_{0.9}$ can be identified with that CrB-type compound with the consequent replica of its magnetic behavior like the modification of the exchange interaction from FM to AFM between Ce-*nn* moments. Once the AFM interaction sets on around Ag

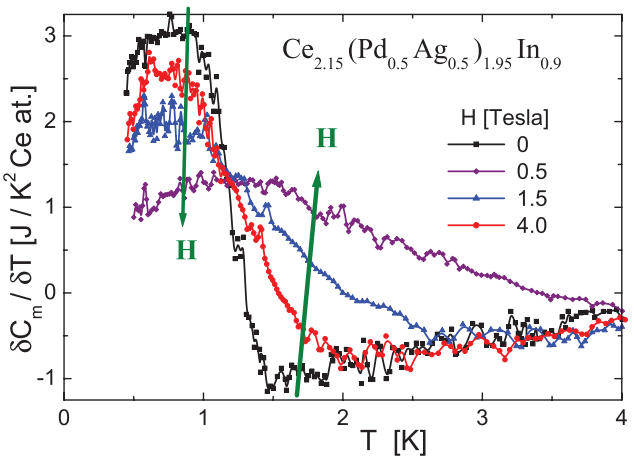


**Figure 9.** Temperature derivative of specific heat at different applied fields showing the decreasing contribution around 1 K and a growing contribution at higher temperature.

dopants, the triangular configuration between Ce-*nn* leads to a magnetic frustration. These features place frustration as the most likely scenario to explain the lack of magnetic signal in the arising $T^*$ anomaly.

Moreover, since the same configuration occurs on the mirror Ce-triangle respect to the Ag atom position (see figure 8(b)) the Pd/Ag substitution affects both neighboring planes simultaneously. This propagation of the AF interaction explains why the FM component practically smears out with 50% of Ag concentration.

Further support that frustration is responsible for the peculiar behavior of this system is provided by magnetic field effects. Since frustrated moments have no preferential they become progressively aligned by applied magnetic field, somehow moving counterclockwise to the Ag concentration driven effect. To properly appreciate this effect on the specific heat, the results of the measurements are presented through its derivative ($\partial C_m/\partial T$) in figure 9. There, one can observe the decrease of the intensity of the maximum slightly below 1 K, but without change in the temperature position up to 4 T. Coincidentally, a clear contribution arises at $T > 1.2$ K. This is an indication for a reversed transference of degrees of freedom, now from the '1 K' anomaly to the FM component.

### 3.2. Entropy bottleneck

While frustration may explain the nature of the '1 K' anomaly, characterized by the absence of magnetic response, its origin remains the open question. In order to face this aspect, one may focus into three features: (i) the low characteristic energy $k_B T^* \propto 1$ K, (ii) the constant value of $T^*$ (i.e. independent of Ag concentration) and (iii) the magnitude of the maximum, which is proportional to the involved fraction of degrees of freedom.

A relevant feature of this anomaly is the strong increase of the density of excitations as $T$ decreases towards $T^*$, reflected in the divergent $C_m(T)/T$ as it is evidenced in figure 10 for sample $x = 0.5$. It is evident that the thermal dependence of the paramagnetic region cannot be sustained down

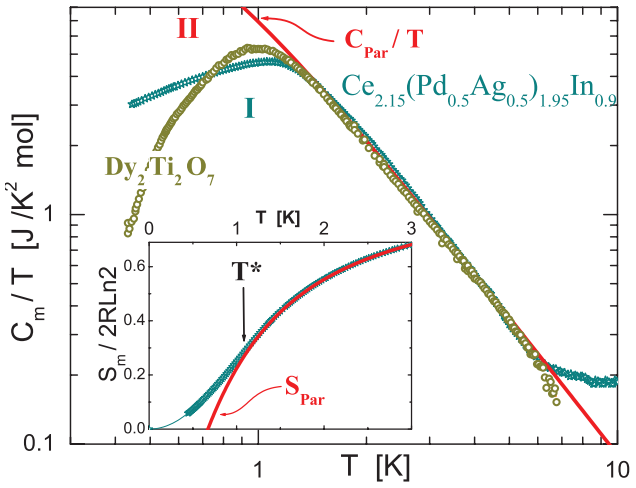


**Figure 10.** Comparison between $C_m/T$ of $x = 0.5$ and $Dy_2Ti_2O_7$ Spin Ice in a double logarithmic representation, where $C_{Par}/T$ indicates a fitting curve, see the text. The region labelled as 'I' indicates the area representing $S_m = \int C_m/T \times dT \leqslant R \ln 2$, whereas 'II' represents $S_{Par} \geqslant R \ln 2$. Inset: low temperature entropy behavior ($S_m$) of the $x = 0.5$ alloy and $S_{Par}$ (continuous curve) evaluated from the $C_{Par}/T$ function. Notice that $S_m$ is normalized by 2Rln 2 because one formula unit involves two Ce atoms.

to $T = 0$ because of its continuous increase (represented by the curve $C_{Par}/T$) would require an amount of entropy $S_{Par} = \int C_{Par}/T \times dT$ (region 'II' in figure 10) that exceeds the $R \ln 2$ limit provided by the doublet GS. To dodge this *entropy bottleneck* [2], the minimum of the free energy of the system slides into an alternative trajectory to allow to fulfill the $S_m \leqslant R \ln 2$ condition imposed by the third law of thermodynamics (represented as region 'I' in figure 10).

In order to analyze in detail the effect of this thermodynamic constraint, we have fitted the experimental result at $T > T^*$ with a function extracted from a heuristic formula $C_{Par}/T = D/(T^Q + E)$ [2] that allows to compare the thermal dependence of a number of heavy fermion compounds. The applicability of this function is evidenced in the comparison between the measured $C_m/T(T)$ of sample $x = 0.5$ and that of the exemplary Spin Ice $Dy_2Ti_2O_7$ [22] that exhibits a clear coincidence. By applying the fit presented in figure 10 (with $D = 9$ J mol$^{-1}$, $Q = 2$ and $E = 0.3$ K$^2$) one may evaluate the excess of entropy required by a model system whose $C_m/T(T)$ keeps growing below $T^*$ with the same temperature dependence like at the $T > T^*$ range. In that case one finds that the entropy associated to $C_{Par}/T$ (i.e. $S_{Par} = \int D/(T^Q + E) \times dT$) nearly doubles the $R \ln 2$ physical limit if the fitted function is extrapolated down to $T = 0$.

A complementary analysis can be done looking how the entropy behaves at the $T \to 0$ limit. The inset in figure 10 shows the $S_m(T)$ evolution with an initial positive curvature related to the increasing $C_m(T)/T$ at $T < T^*$. Focusing on the $T > T^*$ range, one may illustrate the occurrence of an *entropy bottleneck* by tracing $S_{Par}(T < T^*)$ (red curve in the inset) that reaches zero at finite ($T > 0$) temperature. This marks the temperature at which the entropy, evaluated according the $C_{Par}(T)/T$ dependence, would exceed the available entropy $R \ln 2$ of the doublet GS. A further increase of $C_m(T)/T$ following that $C_{Par}(T)/T$ dependence implies a violation of the third law of thermodynamics because $S_{Par}$ extrapolate to negative values. Since the negative curvature of $S_{Par}(T)$ in the paramagnetic range (i.e. $T > T^*$) leads to an unphysical behavior, the change of curvature shown by $S_m(T < T^*)$ corresponds to an allowed trajectory of the entropy ending at $S_m \geqslant 0$ at $T = 0$. This change of curvature of $S_m(T)$ at $T \approx T^*$ is a consequence of a thermodynamic law, i.e. it is not driven by standard magnetic interactions but by thermodynamic constraints.

This fact does not mean that frustrated interactions are suppressed. On the contrary, they participate in the definition of the alternative GS that stabilizes the magnetic system below $T^*$. As expected, this change in the GS character implies a change in the minimum of the free energy ($G_{min}$), which is reflected in the discontinuity observed in the $\partial C_m/\partial T$ derivative (at $H = 0$) shown in figure 9. Such a discontinuity in the third derivative of the free energy (i.e. $\partial^3 G/\partial T^3$) reveals the third order nature of the transition that allows to dodge the 'entropy bottleneck' produced by the $C_{Par}/T$ divergency at $T \to 0$. Therefore, the thermodynamic constraint acts on the frustrated character of the interactions by continuously driving them into an alternative configuration (or $G_{min}$) which is recognized by the $C_m(T < T^*)/T$ decrease. Such temperature dependence is related to the development of some type of order parameter built up by the reoriented interactions. The same scenario applies to a number of other compounds [2] and particularly to the well known Spin Ice $Dy_2Ti_2O_7$. In this case, the stronger $C_m(T < T^*)/T$ slope may indicate another type of alternative configuration or simply makes evident the single-crystal character of the measured sample.

## 4. Conclusions

This FM Ce-system shows a decreasing $T_C(x)$ with the associated degrees of freedom decreasing by Pd/Ag substitution with a critical concentration extrapolated to $x_{cr} \approx 0.6$. No quantum critical point can be claimed in this system because $T_C$ reaches zero vanishing FM degrees of freedom, i.e. the FM component vanishes as $T \to 0$. In this extended investigation we confirm the progressive transference of those degrees of freedom to a non magnetic component that emerges as an anomaly centered at a temperature $T^* \approx 1$ K which is not Ag concentration dependent. The lack of magnetic signal from this '1 K' component is now confirmed in more than one Ag concentration as due to the growing of AFM-frustration occurring among the Ce-neighbors of Ag atoms. Such an AFM character arises from the fact that substitution of Pd 'hole-like' atoms by Ag 'electron-like' reverses the sign of $J_{RKKY}$ exchange between Ce-*nn*. The triangular coordination of Ce magnetic atoms around Ag atoms provides the geometrical condition for such a behavior.

The present interpretation of the results is based on the fact that the $C_m(T^*)/T$ anomaly originates in a thermodynamic constraint and not in standard magnetic interactions between robust magnetic moments. To explain its emergence and its concentration independent $T^* \approx 1$ K temperature, the concept

of *entropy bottleneck* is introduced. The fact that the total amount of excitations (evaluated as $\propto S_m$) would exceed the available degrees of freedom for a doublet GS at finite temperature, compels $S_m(T)$ to search for an alternative thermodynamic trajectory according to the third law of thermodynamics because $S_m \geqslant 0$ as $T \to 0$. Therefore, this system emerges as an original example of *tuned frustration* that builds up from a FM lattice. Further insight into the microscopic details of the GS nature of this system requires from $\mu$SR spectroscopy and neutron scattering investigations.

## Acknowledgments

This work was performed in the frame of the VI Executive Programme of Scientific and Technological Cooperation between Argentina and Italy (2014-2016).

## References

[1] Gruner T, Jang D, Steppke A, Brando M, Ritter F, Krellner C and Geibel C 2014 *J. Phys.: Condens. Matter* **26** 485002
Jang D, Gruner T, Steppke A, Mistsumoto K, Geibel C and Brando M 2015 *Nat. Commun.* **8** 8680
[2] Sereni J G 2015 *J. Low Temp. Phys.* **179** 126
[3] Taufour V, Hodovanets H, Kim S K, Bud'ko S L and Canfield P C 2013 *Phys. Rev.* B **88** 195114
[4] Sereni J G 1991 *Handbook on the Physics and Chemistry of Rare Earths* vol 15, ed K A Gschneidner Jr and L Eyring (Amsterdam: Elsevier) ch 98, pp 1–59
[5] Löhneysen H V, Rosch A, Vojta M and Wölfle P 2007 *Rev. Mod. Phys.* **79** 1015
[6] Stewart G R 2006 *Rev. Mod. Phys.* **73** 797
Stewart G R 2001 *Rev. Mod. Phys.* **78** 743
[7] Lacroix C 2010 *J. Phys. Soc. Japan* **79** 011008
[8] Ramirez A P 1994 *Annu. Rev. Mater. Sci.* **24** 453
[9] Kim M S and Aronson M C 2011 *J. Phys.: Condens. Matter* **23** 164204
[10] Kim M S, Bennett M C and Aronson M C 2008 *Phys. Rev.* B **77** 144425
[11] Giovannini M *et al* 2000 *Phys. Rev.* B **61** 4044
[12] Sereni J G, Giovannini M, Gómez Berisso M and Saccone A 2011 *Phys. Rev.* B **83** 064419
[13] Sereni J G, Giovannini M, Gomez Berisso M and Gastaldo F 2015 *Phys. Proc.* **75** 390
[14] Hiroi Z, Matsuhira K and Ogata M 2003 *J. Phys. Soc. Japan* **72** 3045–8
[15] Sereni J G 2016 *Magnetic Systems: Specific Heat* (*Materials Science and Materials Engineering*) ed S Hashmi (Oxford: Elsevier) pp 1–13
[16] Tari A 2003 *The Specific Heat of Matter at low temperatures* (London: Imperial College Press)
[17] Mydosh J A 1993 *Spin Glasses: an Experimental Introduction* (London: Taylor)
[18] Sereni J G, Pedrazzini P, Gómez Berisso M, Chacoma A, Encina S, Gruner T, Caroca-Cananles N and Geibel C 2015 *Phys. Rev.* B **91** 174408
[19] Sereni J G, Giovannini M, Gómez Berisso M and Saccone A 2012 *J. Phys.: Conf. Ser.* **391** 012062
[20] Kiessling R 1950 *Acta Chem. Scand.* **4** 209
[21] Kappler J P, Besnus M J, Trovarelli O and Sereni J G 1996 *Z. Phys* B **101** 29
[22] Unpublished results on a single crystalline sample provided by S Grigera 2008 Universidad Nacional de La Plata, Argnetina